Deleersnijder, E., & Scherpereel, C. (2026). *Kuwait Bay: an attempt at explaining why the mean residence time and its standard deviation are almost equal to each other at any location*. Working note, 33 pages, available at URL https://hdl.handle.net/2078.5/276619

Kuwait Bay: an attempt at explaining why the mean residence time and its standard deviation are almost equal to each other at any location

Eric Deleersnijder[1], UCLouvain, IMMC[2] & ELI[3], Louvain-la-Neuve, Belgium

Colin Scherpereel[4], UCLouvain, ELI, Louvain-la-Neuve, Belgium

31 May 2026

Contents

Keywords: Persian Gulf, Kuwait Bay, SLIM, CART, partial differential problem, water renewal, one-dimensional diffusive model, Green's function, residence time, residence time distribution function, standard deviation of the residence time

[1] mailto:eric.deleersnijder@uclouvain.be • http://www.ericd.be
[2] https://www.uclouvain.be/en/research-institutes/immc (last viewed on 2 May 2026)
[3] https://www.uclouvain.be/en/research-institutes/eli (last viewed on 2 May 2026)
[4] mailto:colin.scherpereel@uclouvain.be

Abstract. Using a Lagrangian particle tracker, Scherpereel et al. (*Mar. Pollut. Bull.*, 2025) computed the position-dependent mean residence time in Kuwait Bay. Additional numerical results (first presented herein) indicate, quite surprisingly, that at any point of the domain of interest the standard deviation of the residence time is almost equal to the mean residence time. We develop a one-dimensional, purely diffusive model aimed at idealising transport processes in Kuwait Bay. We calculate the relevant Green's function and derive analytical expressions of various timescales. The idealised mean residence time and its standard deviation are rather close to each other, leading us to assume that transport processes are of a diffusive nature at the scale of Kuwait Bay. Many aspects of the idealised model are explored in detail and, presumably, a few novel results are established. We also outline a more elaborate analytical model representing a variety of diffusive features in semi-enclosed domains, ranging from the well-mixed box to the idealised Kuwait Bay model — depending on the ratio of the timescale related to mixing within the domain to the timescale controlling the outward flux through the open boundary.

Introduction

Following the work of Scherpereel et al. (2025), the present working note aims to investigate additional aspects of the water residence time distribution in Kuwait Bay. The latter is a meso-tidal, semi-enclosed, coastal basin located at the northwestern end of the Arabian/Persian Gulf (Figure 1). It is characterised by shallow waters, with an average depth of order 5 m, high salinity, intense evaporation due to an arid regional climate, and complex shoreline features related to recent land reclamation and coastal infrastructure developments (Alosairi and Pokavanich 2017). The Bay spans an area of 737 km^2, delimited by a 19.3-km-long open boundary with the Gulf. Water circulation in the Bay is mainly driven by tides and winds (Alosairi et al. 2018, Yamamoto et al. 2022). It exhibits a significant seasonal variability due to shifts in the prevailing wind regimes, from strong, persistent (up to 40-70 km/h) northwesterly Shamal winds in winter and summer, to other less pronounced regimes, including the Kaus winds during winter and spring (Pous et al. 2013).

Scherpereel et al. (2025) examined the spatial and temporal patterns of water residence time within the Bay, with a particular emphasis on their seasonal variability and the influence of newly implemented coastal infrastructures. To this end, they used a forward-in-time Lagrangian particle-tracking approach based on a hydrodynamic simulation of the Bay performed by the depth-averaged, barotropic version of the coastal ocean model SLIM[5] over the year 2018. This method involves releasing a large number of virtual particles in each triangle of the unstructured mesh covering the Bay and tracking them until they exit it through the eastern mouth, without considering their potential return. The same methodology has been applied hereinafter, focusing on the distribution of residence time values within each triangular element. Despite being subject to strong tides, water circulation in the Bay exhibits

[5] SLIM: Second-generation Louvain-la-Neuve Ice-ocean Model, http://www.slim-ocean.be (last viewed on 2 May 2026)

numerous small-scale coherent structures, including vortices and filaments (see Figures 5 and 6 of Scherpereel et al. 2025), whose cumulative effect enhances mixing and, hence, supports the hypothesis that transport processes could be modelled as diffusion at the scale of the Bay.

The residence time and its standard deviation are almost equal to each other (Figure 2). Providing a tentative explanation of this thought-provoking similarity is the objective of the present working note.

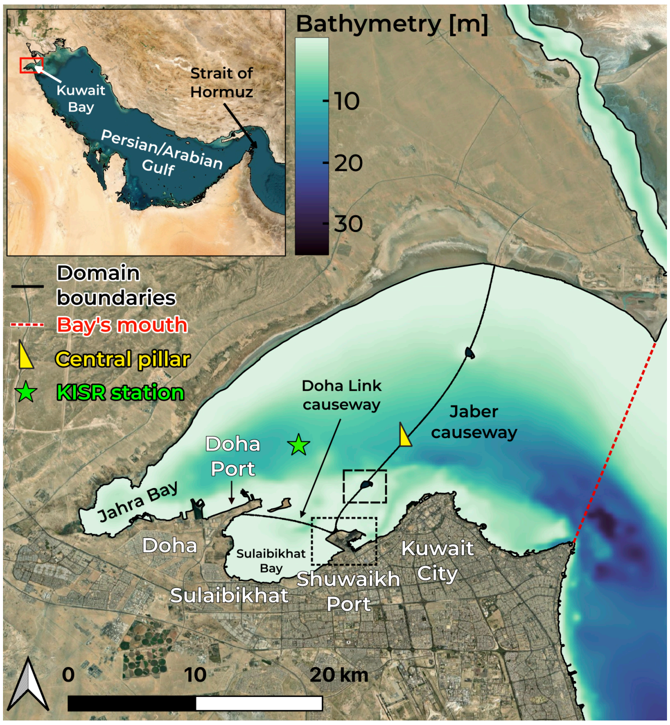

Figure 1. Bathymetry of Kuwait Bay. The red, dotted line is the open boundary of the tracer transport numerical model of Scherpereel et al. (2025). Adapted from Figure 1 of Scherpereel et al. (2025).

One-dimensional, purely diffusive model

Based on the abovementioned considerations, we will build a highly idealised model of Kuwait Bay admitting analytical solutions. Tracer (including water particles[6]) transport is dealt with by means of a one-dimensional, purely diffusive model. If t and x denote the time and a space coordinate, the space-time domain of interest is defined as follows: $0 \le t < \infty$ and $0 \le x \le L$. The $x = 0$ boundary is impermeable, whilst the other end of the domain $(x = L)$ is

[6] In general, water particles move under the influence of advective and diffusive processes. However, the former phenomena are disregarded in the present study. A water particle should not be mistaken for a water parcel, which is an elemental control volume whose velocity is that of the water and is not directly impacted by diffusive processes. Additional pieces of information may be found in Deleersnijder et al. (2001), Deleersnijder 2017, Deleersnijder (2020), or Lucas and Deleersnijder (2020).

open (Figure 3). The latter is the interface between the idealised Kuwait Bay and the Persian Gulf, the role of which is not taken into account explicitly hereinafter.

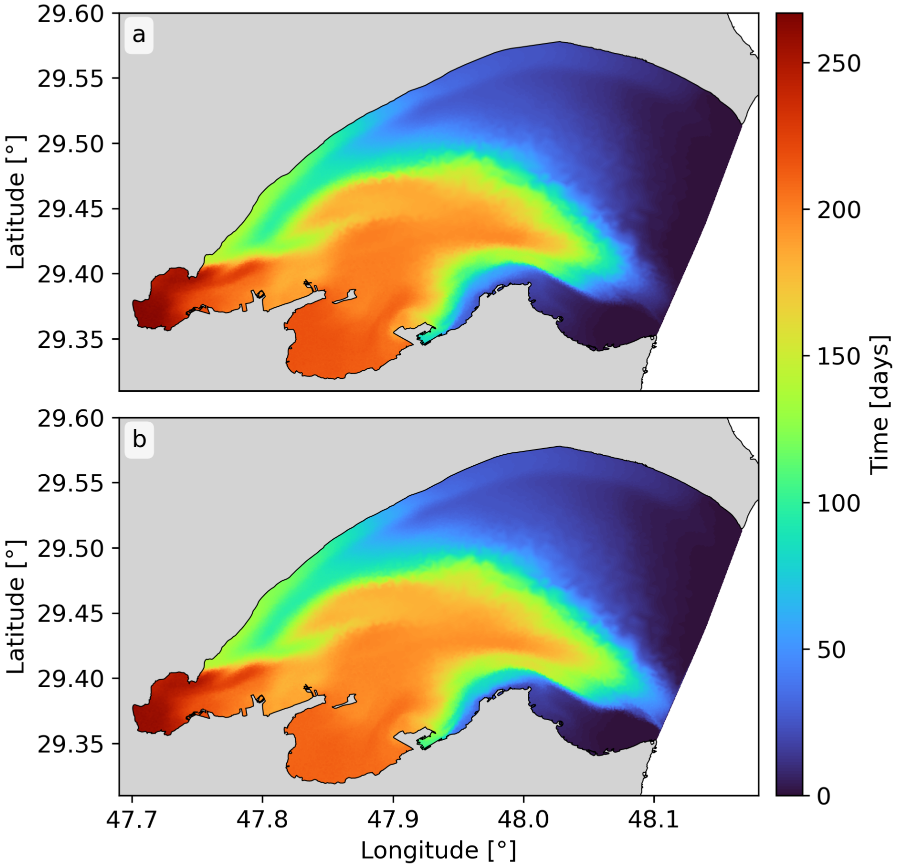

Figure 2. Mean (a) and standard deviation (b) of residence time distribution in Kuwait Bay in 2018, obtained from a numerical simulation with more than 1 billion particles (about 10 000 particles per triangle). A particle is discarded at the instant it hits the open boundary and the time needed for this particle to travel from its starting point to the open boundary is its residence time.

Concentration $C(t,x)$ of particles of a passive tracer initially located in the domain of interest is governed by partial differential equation

$$\frac{\partial C}{\partial t} = K \frac{\partial C}{\partial x^2} \tag{1}$$

where positive constant K is the along-bay diffusivity. This equation is to be dealt with under initial condition

$$\left[C(t,x)\right]_{t=0} = C^0(x) \geq 0 \tag{2}$$

where $C^0(x)$ denotes the concentration prevailing at the initial instant $(t=0)$. The impermeability condition of the $x=0$ boundary reads

$$\left[K\frac{\partial C}{\partial x}\right]_{x=0} = 0 \tag{3}$$

It is assumed that every particle reaching the open boundary ($x = L$) leaves the domain once and for all, leading to boundary condition

$$\left[C(t,x)\right]_{x=L} = 0 \tag{4}$$

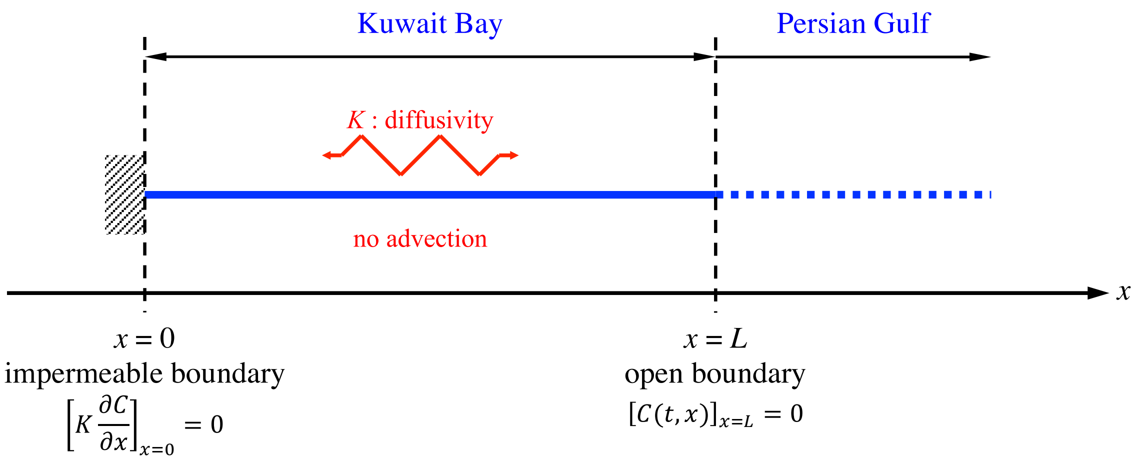

Figure 3. Illustration of the key ingredients of the analytical model aimed at representing tracer concentration and related diagnoses in a highly simplified, one-dimensional approach to transport processes in Kuwait Bay and fluxes toward the Persian Gulf, which is not explicitly taken into account herein. The concentration of a passive tracer, which may be tagged water particles, is denoted $C(t,x)$, where t denotes the time, whilst x is the distance to the impermeable boundary of the domain of interest.

The solution to partial differential problem (1)-(4) reads (e.g., Carslaw 1921)

$$C(t,x) = \sum_{n=1}^{\infty} C_n\, e^{-Kk_n^2 t}\cos(k_n x) \tag{5}$$

with

$$C_n = \frac{2}{L}\int_0^L C^0(x)\cos(k_n x)\,dx \tag{6}$$

and

$$k_n = \frac{\pi}{L}(n-1/2) \tag{7}$$

The amount of tracer present in the domain of interest, which for the sake of simplicity will be referred to as the "tracer mass", is

$$m(t) = \int_0^L C(t,x)\,dx \tag{8}$$

Substituting (5) into (8) yields

$$m(t) = \frac{L}{\pi}\sum_{n=1}^{\infty}\frac{(-1)^{n+1}C_n}{(n-1/2)}e^{-Kk_n^2 t} \tag{9}$$

Then, we easily obtain

$$m(0) = \frac{L}{\pi}\sum_{n=1}^{\infty}\frac{(-1)^{n+1}C_n}{(n-1/2)} \tag{10}$$

and

$$m(t) \sim \frac{2L}{\pi}\sum_{n=1}^{\infty}C_1\, e^{-Kk_1^2 t} \quad , \quad \frac{Kt}{L^2}\to\infty \qquad (11)^7$$

hence

$$\lim_{t\to\infty}\left[t^{\alpha}m(t)\right] = 0 \quad (\alpha \geq 0) \qquad (12)^8$$

The timescale characterising the decrease of $m(t)$ is $1/(Kk_1^2) \approx 4L^2/(\pi^2 K) \approx 0.4\times L^2/K$ (e.g., Deleersnijder 2019a). Accordingly, L^2/K may be viewed as the key timescale of the transport problem under consideration. This is unsurprising since L^2/K is the only combination of the dimensional parameters at hand that has the physical dimension of a timescale.

Combining (1), (3) and (8) readily leads to

$$\frac{dm}{dt} = \left[K\frac{\partial C}{\partial x}\right]_{x=L} \tag{13}$$

Since initial concentration $C^0(x)$ is non-negative, then $C(t,x)$ may be seen to be non negative (Appendix A). According to boundary condition (4), the concentration is zero on the open boundary. Therefore, $\left[\partial C/\partial x\right]_{x=L}$ is non positive, implying that $m(t)$ cannot increase. In fact, in most, if not all cases, the tracer mass strictly decreases and tends to zero in the limit $t\to\infty$ in any circumstance.

Diagnostic timescales

The mass of the tracer particles leaving the domain of interest during time interval $[t, t+\Delta t]$ tends to $(-dm/dt)\Delta t$ in the limit $\Delta t\to 0$. Time t is the residence time of these tracer particles, i.e., the time needed for them to reach the open boundary (e.g., Bolin and Rodhe 1973, Zimmerman 1976, Takeoka 1984, Zimmerman 1988, Delhez et al. 2004). The mean

[7] In the limit $Kt/L^2\to\infty$, $e^{-Kk_1^2/t} >> e^{-Kk_2^2/t} >> e^{-Kk_3^2/t}\ldots$, because $k_1 < k_2 < k_3\ldots$, implying that, in the long run, the $n=1$ mode becomes dominant and the other ones tend to be negligible.

[8] This is based on the following (well known) property: $\lim_{t\to\infty} t^{\alpha}e^{-\beta t} = 0 \ (\beta > 0)$.

residence time of all the tracer particles under consideration, is usually defined as a mass-weighted average of the residence times of the outgoing elemental masses, i.e.,

$$\Theta = \frac{1}{m(0)} \lim_{\Delta t \to 0} \sum_{t=0}^{\infty} t \left(-\frac{dm}{dt} \right) \Delta t = -\frac{1}{m(0)} \int_0^{\infty} t \frac{dm}{dt} dt \tag{14}$$

This expression transforms to

$$\Theta = -\frac{\overbrace{\left[t\, m(t) \right]_{t=\infty}}^{=0,\text{ see (12)}} - \overbrace{\left[t\, m(t) \right]_{t=0}}^{=0}}{m(0)} + \frac{1}{m(0)} \int_0^{\infty} m(t)\, dt \tag{15a}$$

which simplifies to

$$\Theta = \frac{1}{m(0)} \int_0^{\infty} m(t)\, dt \tag{15b}$$

It must be underscored that formula (15b) is valid whatever the initial tracer concentration (e.g., Takeoka 1984).

The residence time is concerned with the future evolution of the particles under study, whereas the age looks into their past as it is a measure of an elapsed time. At the core of the age theory that is part of CART[9] is the age distribution function (e.g., Delhez et al. 1999). It may be regarded as the histogram of the ages of the particles under consideration, which, in its most comprehensive formulation, is a function of time, position and the age itself — as an independent variable. This distribution function was seen to be key for the formulation of consistent boundary conditions (Deleersnijder et al. 2020) and instrumental in the interpretation of model results (e.g., Delhez and Deleersnijder 2002, Dewals et al. 2020, Dewals et al. 2024). To develop the residence time theory within the framework of CART, Delhez et al. (2004) also resorted to a kind of distribution function. A very simplified and slightly modified version of it is introduced below.

If the mean residence time is not the only diagnostic quantity we are interested in, then it is appropriate to first introduce the residence time distribution function, $\mu(t)$. The latter is defined as follows: the fraction of the tracer particles leaving the domain of interest during time interval $[t, t+\Delta t]$ tends to $\mu(t)\Delta t$ in the limit $\Delta t \to 0$. In light of the considerations above, the residence time distribution function (i.e., the histogram of the residence times of the tracer particles under study) is

$$\mu(t) = -\frac{1}{m(0)} \frac{d}{dt} m(t) \tag{16}$$

Substituting (9) into (16) yields

$$\mu(t) = \frac{1}{m(0)} \frac{\pi K}{L} \sum_{n=1}^{\infty} (-1)^{n+1} (n - 1/2) C_n\, e^{-K k_n^2 t} \tag{17}$$

Moments of the residence time distribution function, i.e.,

[9] CART = <u>C</u>onstituent-oriented <u>A</u>ge and <u>R</u>esidence time <u>T</u>heory, http://www.cartdiagnoses.be (formerly http://www.climate.be/cart) (lat viewed on 31 May 2026)

$$\gamma_j = \int_0^{\infty} t^j \mu(t)\, dt \quad (j = 0,1,2,...) \tag{18}$$

carry statistical information about the behaviour of the tracer particles under study. Combining (17) and (18), we obtain

$$\gamma_j = \frac{1}{m(0)} \frac{j!\, L^{1+2j}}{\pi^{1+2j} K^j} \sum_{n=1}^{\infty} \frac{(-1)^{n+1} C_n}{(n-1/2)^{1+2j}} \tag{19}$$

The zeroth-order moment of the distribution function is identically equal to unity. Indeed, integrating (16) over time yields

$$\gamma_0 = \int_0^{\infty} \left[-\frac{1}{m(0)} \frac{d}{dt} m(t) \right] dt = -\frac{\overbrace{\left[m(t)\right]_{t=\infty}}^{=0,\,\text{see (12)}} - \left[m(t)\right]_{t=0}}{m(0)} = 1 \tag{20}$$

Most, if not all distribution functions are designed such that they satisfy a similar constraint. On the other hand, the mean residence time reads

$$\Theta = \gamma_1 = \int_0^{\infty} t\mu(t)\, dt = \frac{1}{m(0)} \frac{L^3}{\pi^3 K} \sum_{n=1}^{\infty} \frac{(-1)^{n+1} C_n}{(n-1/2)^3} \tag{21}$$

whilst the variance is

$$\sigma^2 = \int_0^{\infty} (t-\Theta)^2 \mu(t)\, dt = \gamma_2 - \Theta^2 \tag{22}$$

The standard deviation, i.e.,

$$\sigma = \sqrt{\gamma_2 - \Theta^2} \tag{23}$$

is usually regarded as a measure of the "width" of the distribution function.

Illustration: residence time of the original water

The way Scherpereel et al. (2025) computed the residence time turns out to be in agreement with some aspects of the multi-faceted approach to water renewal assessment outlined by Gourgue et al. (2007), which has ben adopted by, e.g., de Brye et al. (2012), Deleersnijder (2019b), Pham Van et al. (2020) and Deleersnijder (2026). The concept of water renewal refers to all the processes by which water initially present in the domain of interest (i.e., the original water) is progressively replaced by water originating from its environment (i.e., the renewing water). Such phenomena significantly impact ecology, pollutant dispersal, sediment transport, etc. Therefore, quantifying the rate at which water renewal takes place is considered as an important step in many eco-hydrodynamic studies.

Gourgue et al. (2007) suggested tracking the original and renewing waters in the Eulerian framework[10] and calculating related timescales. The latter are chiefly the residence time of the

[10] This can also be done by means of a Lagrangian method (e.g., van Sebille et al. 2018, Heemink et al. 2022).

original water (i.e., the time needed to leave the domain)[11] and the age of the renewing water (i.e., the time elapsed since entering the domain). The aforementioned water types are treated as passive tracers[12].

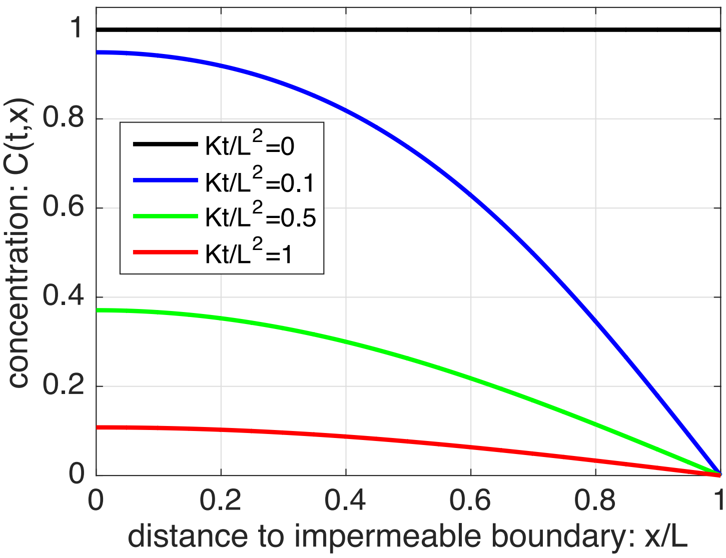

Figure 4. Concentration of the original water according to (24) at different instants as a function of the distance to the impermeable boundary of the domain of interest. Clearly, L^2/K is the order of magnitude of the timescale characterising the transport of the original water out of the domain of interest.

The original water is initially homogeneous in the domain of interest, i.e., $C^0(x)=1$. Then, (6) leads to $C_n = 2(-1)^{n+1}/[\pi(n-1/2)]$ so that the original water concentration reads (Figure 4)

$$C(t,x) = \frac{2}{\pi}\sum_{n=1}^{\infty}\frac{(-1)^{n+1}}{n-1/2}e^{-Kk_n^2 t}\cos(k_n x) \tag{24}$$

Then, using (9), the mass of original water present in the domain is readily seen to be (Figure 5)

$$m(t) = \frac{2L}{\pi^2}\sum_{n=1}^{\infty}\frac{e^{-Kk_n^2 t}}{(n-1/2)^2} \tag{25}$$

with

$$m(0) = \frac{2L}{\pi^2}\sum_{n=1}^{\infty}\frac{1}{(n-1/2)^2} = L \tag{26}$$

---

[11] A variant of the residence time, namely the exposure time, allows taking into account the fact that original water particles may re-enter the domain of interest after leaving it for the first time (e.g., Monsen et al. 2002, Delhez et al. 2004, de Brauwere et al. 2011, Andutta et al. 2016).

[12] Treating a water type as a passive tracer is long-standing practice in numerical oceanography (e.g., Cox 1989, Hirst 1999, Goosse et al. 2001, Deleeersnijder et al. 2002, Haine and Hall 2002, Meier 2005).

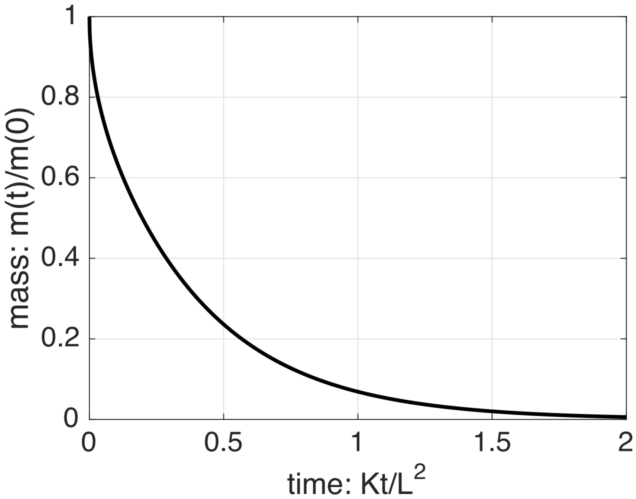

Figure 5. Mass of the original water according to (25) as a function of time, suggesting that L^2/K is the order of magnitude of the timescale characterising the decrease of $m(t)$.

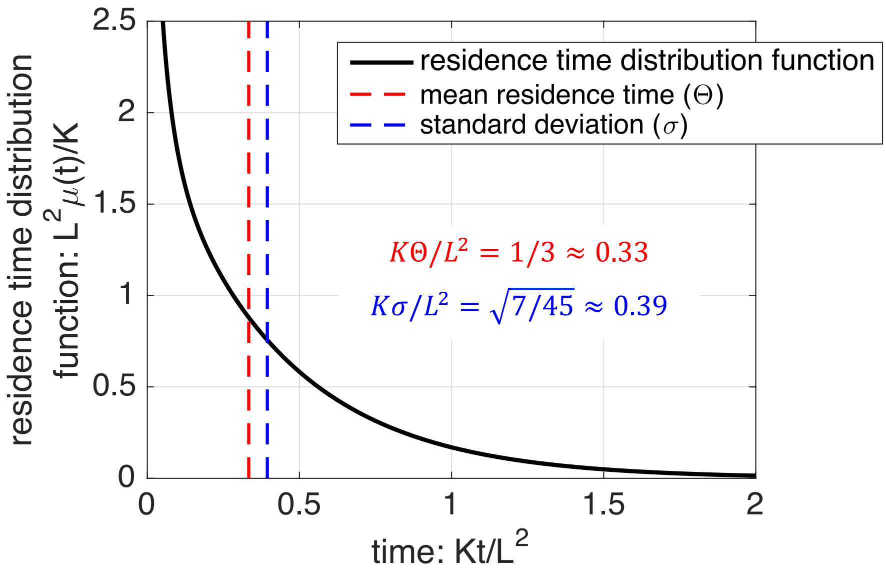

Figure 6. Residence time distribution function $\mu(t)$ (black, solid curve). The dotted red line and the blue one indicate the value of mean residence time Θ and standard deviation σ, respectively. In the limit $t \to 0$, the residence distribution function is singular, for it is proportional to $1/\sqrt{t}$. Fortunately, this singularity is integrable[13]. It is a physical consequence of diffusion (e.g., Primeau and Holzer 2006, Hall et al. 2007).

[13] Integral $\int_0^t 1/\sqrt{t'}\,dt' = 2\sqrt{t}$ is not singular in the limit $t \to 0$!

In accordance with (17), the residence time distribution function is (Figure 6)

$$\mu(t) = \frac{2K}{L^2} \sum_{n=1}^{\infty} e^{-K k_n^2 t} \tag{27}$$

and its moments read

$$\gamma_j = \frac{2\, j!\, L^{2j}}{\pi^{2+2j} K^j} \sum_{n=1}^{\infty} \frac{1}{(n-1/2)^{2+2j}} = \frac{(2^{3+2j}-2)\, j!\, L^{2j}}{\pi^{2+2j} K^j} \zeta_{ER}(2+2j) \quad (j=0,1,2,...) \tag{28}$$

where ζ_{ER} denotes the Euler-Riemann zeta function. Following (20), the zeroth-order moment is identically zero:

$$\gamma_0 = \frac{2}{\pi^2} \sum_{n=1}^{\infty} \frac{1}{(n-1/2)^2} = 1 \tag{29}$$

The first-order moment is the mean residence time of the original water

$$\Theta = \gamma_1 = \frac{2L^2}{\pi^4 K} \sum_{n=1}^{\infty} \frac{1}{(n-1/2)^4} = \frac{L^2}{3K} \approx 0.33 \times \frac{L^2}{K} \tag{30}$$

whilst the second-order moment

$$\gamma_2 = \frac{4L^4}{\pi^6 K^2} \sum_{n=1}^{\infty} \frac{1}{(n-1/2)^6} = \frac{4L^4}{15K^2} \tag{31}$$

allows evaluating the variance of the residence time distribution function, i.e.,

$$\sigma^2 = \gamma_2 - \gamma_1^2 = \frac{7L^4}{45K^2} \tag{32}$$

as well as the related standard deviation

$$\sigma = \sqrt{\gamma_2 - \gamma_1^2} = \sqrt{\frac{7}{45}}\frac{L^2}{K} \approx 0.39 \times \frac{L^2}{K} \tag{33}$$

The model at hand comprises only two dimensional parameters, L and K. Therefore, as already pointed out, any timescale based on these parameters must be proportional to L^2/K. It is noteworthy that the mean residence time and the standard deviation are almost equal to each other:

$$\frac{\sigma - \Theta}{\Theta} = \sqrt{\frac{7}{5}} - 1 \approx 0.18 \tag{34}$$

Green's function based solutions

In the previous sections, we have shown how to evaluate timescales related to a passive tracer in a highly idealised, purely diffusive model of Kuwait Bay. The results hold valid irrespective of the initial distribution of the tracer under consideration. However, to derive pointwise timescales, further developments are needed. In this respect, having recourse to the concept of Green's function is instrumental.

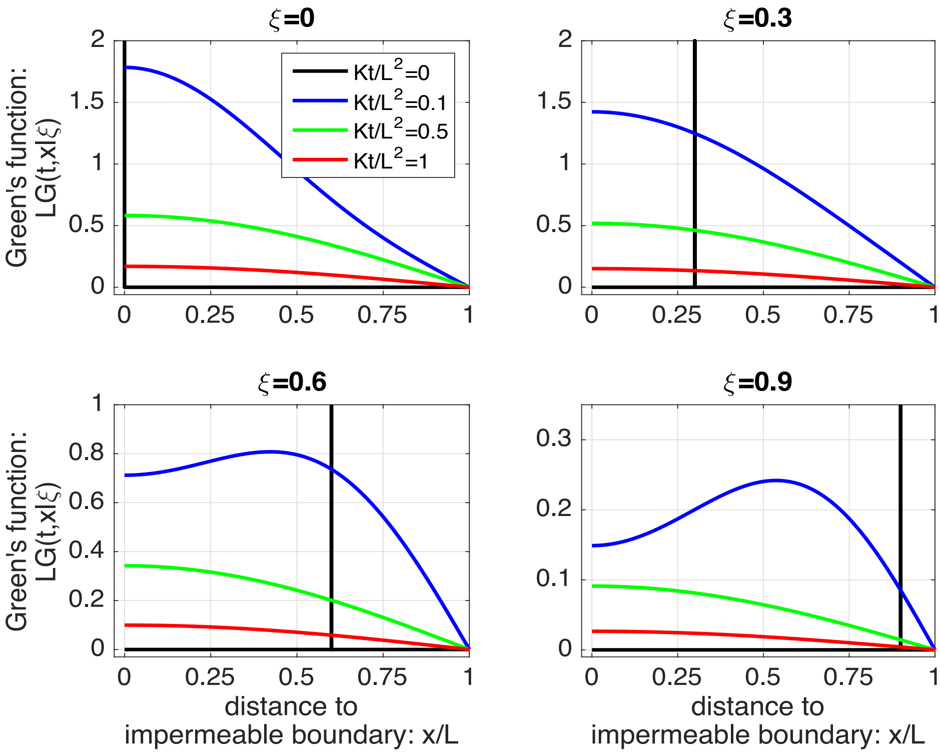

Figure 7. Representation at various instants of Green's function (40) as a function of the distance to impermeable boundary for four values of ξ .

Presumably, Robin Hood is the most famous (fictional or real) character associated with the city of Nottingham, United Kingdom. However, miller and self-taught mathematician George Green (1793-1841)[14] is perhaps the most influential citizen of Nottingham although he is much lesser known by the general public than Robin Hood — and his infamous archenemy, the Sheriff of Nottingham. George Green single-handedly designed a tool (commonly called Green's function, impulse response or transfer function, depending on the domain of application) for solving linear ordinary or partial differential problems (Green 1828) that is still in use nowadays (e.g., Jackson 1962, Duffy 2018, Haine et al. 2025). In 1930, while lecturing at the University of Nottingham, Albert Einstein (1879-1955) declared that Green “was twenty years ahead of his time”[15].

The tracer concentration satisfying partial differential problem (1)-(4) may be derived from the following convolution product

$$C(t,x) = \int_0^L C^0(\xi)G(t,x\,|\,\xi)\,d\xi \tag{35}$$

where $G(t,x\,|\,\xi)$ is the relevant Green's function. The latter is the solution to partial differential problem

[14] https://www.nottingham.ac.uk/physics/about/history/george-green.aspx (last viewed on 26 March 2026)
[15] https://mathshistory.st-andrews.ac.uk/Strick/green.pdf (last viewed on 26 March 2026)

$$\frac{\partial G}{\partial t} = K\frac{\partial G}{\partial x^2} \tag{36}$$

$$\left[G(t,x\,|\,\xi)\right]_{t=0} = \delta(x-\xi) \tag{37}$$

$$\left[K\frac{\partial G}{\partial x}\right]_{x=0} = 0 \tag{38}$$

$$\left[G(t,x\,|\,\xi)\right]_{x=L} = 0 \tag{39}$$

where δ is the Dirac impulse (or delta) function (Appendix B). The Green's function reads (Figure 7, Appendix C)

$$G(t,x\,|\,\xi) = \frac{2}{L}\sum_{n=1}^{\infty} e^{-Kk_n^2 t}\cos(k_n\xi)\cos(k_n x) \qquad (40)^{16}$$

Substituting (40) into (35) yields (5)-(6), as expected. Q.E.D.

The Dirac delta function identically satisfies

$$\int_{-\infty}^{\infty}\delta(\varsigma)\,d\varsigma = 1 \tag{41}$$

implying that its physical dimension is the inverse of that of its argument. Accordingly, in light of (37), the physical dimension of $G(t,x\,|\,\xi)$ is *length*$^{-1}$. The same result could have been deduced from a simple inspection of (35). Clearly, the Green's function dealt with herein cannot be viewed as a tracer concentration. In fact, $G(t,x\,|\,\xi)$ is the response of the partial differential transport problem tackled in this working note to a Dirac impulse located at $x=\xi$, and this impulse response is instrumental in formulating actual tracer concentrations and related diagnoses. Specifically, combining (8), (15b), (35) and (37) yields residence time

$$\Theta = \frac{\int_0^{\infty}\int_0^{L}\int_0^{L} C^0(\xi)G(t,x\,|\,\xi)\,d\xi\,dx\,dt}{\int_0^{L} C^0(x)\,dx} \tag{42}$$

Pointwise diagnoses

Nowadays many studies rely on pointwise diagnoses, which may be derived from a relevant interpretation of convolution product (35). The contribution to this integral of the tracer particles initially located in space segment $[x_s-\Delta x_s/2, x_s+\Delta x_s/2]$ satisfies

[16] The Green's function satisfies Maxwell's reciprocity property, i.e., $G(t,x\,|\,\xi)=G(t,\xi\,|\,x)$. This is typical of purely diffusive (no advection) transport problems (e.g., Deleersnijder 2016, Deleersnijder 2025).

$$\int_{x_s-\Delta x_s/2}^{x_s+\Delta x_s/2} C^0(\xi)G(t,x\,|\,\xi)\,d\xi \sim C^0(x_s)G(t,x\,|\,x_s)\Delta x_s \ , \quad \Delta x_s \to 0 \tag{43}$$

Therefore, in the limit $\Delta x_s \to 0$, (35) is the sum of such elemental contributions. Coordinate x_s may be regarded as the starting point[17] of the aforementioned tracer particles. Expression (42) allows evaluating the residence time of these particles

$$\frac{\displaystyle\int_0^\infty\int_0^L\int_{x_s-\Delta x_s/2}^{x_s+\Delta x_s/2} C^0(\xi)G(t,x\,|\,\xi)\,d\xi\,dx\,dt}{\displaystyle\int_{x_s-\Delta x_s/2}^{x_s+\Delta x_s/2} C^0(x)\,dx} \sim \frac{\displaystyle\int_0^\infty\int_0^L C^0(x_s)G(t,x\,|\,x_s)\Delta x_s\,dx\,dt}{C^0(x_s)\Delta x_s} \tag{44}$$

with $\Delta x_s \to 0$. Asymptotic expression (44) readily simplifies to

$$\theta(x_s) = \int_0^\infty\int_0^L G(t,x\,|\,x_s)\,dx\,dt \tag{45}$$

which may be viewed as the residence time of the tracer particles that are initially located in an elemental control volume located at distance x_s to the impermeable boundary. It is appropriate to term this timescale "pointwise residence time" or "residence time", for short. Combining (42) and (45) yields

$$\Theta = \frac{\displaystyle\int_0^L C^0(x)\theta(x)\,dx}{\displaystyle\int_0^L C^0(x)\,dx} \tag{46}$$

The pointwise residence time can be derived from the Green's function and the mean residence time of tracer particles, irrespective of their initial distribution, is the average weighed by the initial concentration of the pointwise residence time. For instance, the mean residence time of the original water is

$$\Theta = \frac{\displaystyle\int_0^L \theta(x)\,dx}{\displaystyle\int_0^L dx} = \frac{1}{L}\int_0^L \theta(x)\,dx \tag{47}$$

since the initial concentration of the original water is equal to unity, i.e., $C^0(x)=1$.

Formulas (45)-(47) hold valid for most, if not all steady-state, one-dimensional, reactive,

[17] Many studies refer to x_s as the "release point". We believe that this expression is somewhat misleading if it is applied to tracer particles that are present in the domain of interest at the initial instant (e.g., the original water particles). In our humble opinion, the expression "release point" should be reserved to particles that are actually injected into the domain of interest by, e.g., a point source.

linear transport problems provided the relevant Green's function is resorted to. Clearly, the importance of the Green's function cannot be overestimated (e.g., Haine et al. 2025).

For the present highly idealised Kuwait Bay model, the Green's function is formula (40). Substituting this relation into (45) yields the pointwise residence time, i.e.,

$$\theta(x_s) = \frac{2}{L}\int_0^{\infty}\int_0^{L}\sum_{n=1}^{\infty} e^{-Kk_n^2 t}\cos(k_n x_s)\cos(k_n x)\,dx\,dt = \frac{2L^2}{\pi^3 K}\sum_{n=1}^{\infty}\frac{(-1)^n\cos(k_n x_s)}{(n-1/2)^3} \qquad (48a)$$

which simplifies to (Appendix D) (Figure 8)

$$\theta(x_s) = \frac{L^2 - x_s^2}{2K} \qquad (48b)^{18}$$

The average over the domain of this timescale is equal to the mean residence time of the original water (30), i.e.,

$$\langle\theta(x_s)\rangle = \frac{1}{L}\int_0^{L}\theta(x_s)\,dx_s = \frac{L^2}{3K} \approx 0.33\times\frac{L^2}{K} \qquad (49)$$

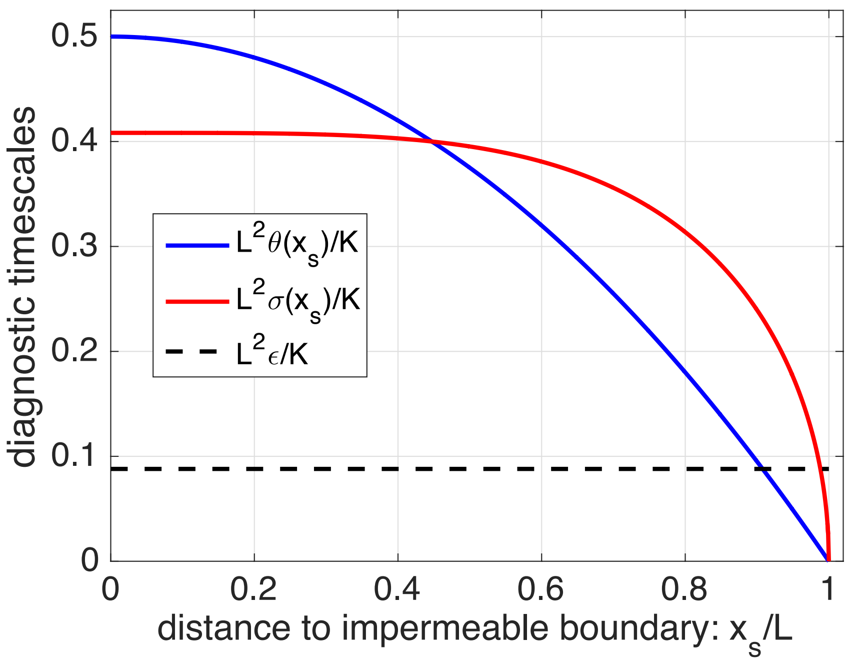

Figure 8. Residence time $\theta(x_s)$ and its standard deviation $\sigma(x_s)$ as a function of distance x_s to the impermeable boundary evaluated by means of formulas (48b) and (58), respectively. The root mean square difference between $\theta(x_s)$ and $\sigma(x_s)$, i.e., ε, is also shown (see (60)).

[18] Dronkers and Zimmerman (1982) derived a similar formula from theoretical developments that are more general (albeit highly concise, and, hence, somewhat difficult to comprehend) than those of the present working note. It this study, it was also seen that (48b) is the steady-state age of water particles defined as the time elapsd since leaving the open boundary. See also Deleersnijder (2011).

Seeking inspiration in (16), the residence time distribution function of the tracer particles initially located in an elemental control volume located at distance x_s to the impermeable boundary is readily seen to be

$$\mu(t,x_s) \;=\; -\frac{\dfrac{d}{dt}\displaystyle\int_0^L G(t,x\,|\,x_s)\,dx}{\displaystyle\int_0^L G(0,x\,|\,x_s)\,dx} \tag{50a}$$

which simplifies to

$$\mu(t,x_s) \;=\; -\frac{d}{dt}\int_0^L G(t,x\,|\,x_s)\,dx \tag{50b}$$

since the integral over the domain of interest of $G(0,x\,|\,x_s)=\delta(x-x_s)$ is identically equal to unity. Relation (50b) holds valid for most, if not all steady-state, one-dimensional, reactive, linear transport problems provided the relevant Green's function is resorted to.

For the present highly idealised Kuwait Bay model, the Green's function is formula (40). Substituting this relation into (50b) yields

$$\mu(t,x_s) \;=\; \frac{2\pi K}{L^2}\sum_{n=1}^{\infty}(-1)^{n+1}(n-1/2)\,e^{-Kk_n^2 t}\cos(k_n x_s) \tag{51}$$

The average over the domain of interest of $\mu(t,x_s)$ reads

$$\langle\mu(t,x_s)\rangle \;=\; \frac{1}{L}\int_0^L \mu(t,x_s)\,dx_s \;=\; \frac{2K}{L^2}\sum_{n=1}^{\infty}e^{-Kk_n^2 t} \tag{52}$$

As expected, this result is equal to (27), the residence time distribution function of the original water.

The moments of the pointwise residence time distribution functions are

$$\gamma_j(x_s) \;=\; \int_0^{\infty} t^j\mu(t,x_s)\,dt \quad (j=0,1,2,\ldots) \tag{53}$$

As expected, the $j=0$ moment is identically equal to unity (Appendix D)

$$\gamma_0(x_s) \;=\; \int_0^{\infty}\mu(t,x_s)\,dt \;=\; \frac{2}{\pi}\sum_{n=1}^{\infty}\frac{(-1)^{n+1}}{n-1/2}\cos(k_n x_s) \;=\; 1 \tag{54}$$

The $j=1$ moment is equal to pointwise residence (48b) (Appendix D),

$$\gamma_1(x_s) \;=\; \int_0^{\infty} t\mu(t,x_s)\,dt \;=\; \frac{2L^2}{\pi^3 K}\sum_{n=1}^{\infty}\frac{(-1)^n\cos(k_n x_s)}{(n-1/2)^3} \;=\; \frac{L^2-x_s^2}{2K} \;=\; \theta(x_s) \tag{55}$$

as it must be. The second-order moment is (Appendix D)

$$\gamma_2(x_s) \;=\; \int_0^{\infty} t^2\mu(t,x_s)\,dt \;=\; \frac{4L^4}{\pi^5 K^2}\sum_{n=1}^{\infty}\frac{(-1)^n\cos(k_n x_s)}{(n-1/2)^5} \;=\; \frac{5L^4-6L^2x_s^2+x_s^4}{12K^2} \tag{56}$$

and, unsurprisingly, its average over the domain of interest, $\langle\gamma_2(x_s)\rangle = 4L^4/(15K^2)$, is equal to the second-order moment of the residence time distribution function of the original water, i.e., relation (31). Then, the variance of the pointwise residence time distribution function reads

$$\sigma^2(x_s) = \int_0^\infty [t-\theta(x_s)]^2 \mu(t,x_s)\,dt = \gamma_2(x_s)-[\theta(x_s)]^2 = \frac{L^4-x_s^4}{6K^2} \tag{57}$$

so that the corresponding standard deviation is (Figure 8)

$$\sigma(x_s) = \sqrt{\frac{L^4-x_s^4}{6K^2}} \tag{58}$$

For obvious reasons, this standard deviation is not equal to (33), the standard deviation related to the time evolution of the original water concentration. The mean over the domain of (58) is

$$\langle\sigma(x_s)\rangle = \frac{1}{L}\int_0^L \sqrt{\frac{L^4-x_s^4}{6K^2}}\,dx_s = \sqrt{\frac{\pi}{384}}\,\frac{\Gamma(1/4)}{\Gamma(7/4)}\,\frac{L^2}{K} \approx 0.36\times\frac{L^2}{K} \tag{59}$$

where Γ denotes the gamma function[19]. This value is very close to the domain-averaged residence time, which, according to (49), is approximately equal to $0.33\times(L^2/K)$.

The root mean square difference between $\theta(x_s)$ and $\sigma(x_s)$ is

$$\begin{aligned}\varepsilon &= \left[\frac{1}{L}\int_0^L [\theta(x_s)-\sigma(x_s)]^2\,dx_s\right]^{1/2} \\ &= \left[\frac{4}{15}-\sqrt{\frac{\pi}{216}}\left(\frac{3\Gamma(5/4)}{\Gamma(7/4)}-\frac{\Gamma(7/4)}{\Gamma(9/4)}\right)\right]^{1/2}\frac{L^2}{K} \approx 0.088\times\frac{L^2}{K}\end{aligned} \tag{60}$$

Next, the residence time and its standard deviation satisfy

$$\langle\theta^2(x_s)-\sigma^2(x_s)\rangle = \frac{1}{L}\int_0^L [\theta^2(x_s)-\sigma^2(x_s)]\,dx_s = 0 \tag{61}$$

At the time of writing, we are not able to provide a physical interpretation of this seemingly remarkable property. Finally, another potentially useful measure of the difference between $\theta(x_s)$ and $\sigma(x_s)$ is

$$\begin{aligned}\left\langle[\theta^2(x_s)-\sigma^2(x_s)]^2\right\rangle^{1/4} &= \left[\frac{1}{L}\int_0^L [\theta^2(x_s)-\sigma^2(x_s)]^2\,dx_s\right]^{1/4} \\ &= \left(\frac{8}{2835}\right)^{1/4}\frac{L^2}{K} \approx 0.23\times\frac{L^2}{K}\end{aligned} \tag{62}$$

Appendix E shows how to evaluate all the moments of the residence time distribution function from the solution of ordinary differential problems without explicitly calculating $\mu(t,x_s)$. Presumably, this method for deriving the moments is simpler than that resorted to above.

---

[19] $\Gamma(z)=\int_0^\infty e^{-\varsigma}\varsigma^{z-1}\,d\varsigma$. See, e.g., https://mathworld.wolfram.com/GammaFunction.html (last viewed on 15 May 2026)

The analytical developments carried out above show that the residence time and its standard deviation are rather close to each other (Figure 8). However, in the numerical model results (Figure 9), these two diagnostic timescales are closer to each other. Indeed, for the analytical developments, the ratio $\varepsilon / \langle \theta(x_s) \rangle$ is approximately equal to 0.27 whilst, for the numerical results, this ratio is about 0.16. The numerical and analytical results show that the standard deviation is greater than the mean residence time in a wide region adjacent to the open boundary of the domain. On the other hand, in the remainder of the domain, the computed mean residence time and standard deviation are very close to each other. The behaviour of the analytical solutions is different. At distance $x_s^* = L/\sqrt{5}$ to the impermeable boundary, the mean residence time and the standard deviation are equal to each other. Then, the following properties are obeyed:

$$\frac{1}{x_s^*} \int_0^{x_s^*} \left[\theta(x_s) - \sigma(x_s) \right] dx_s \approx 0.060 \times \frac{L^2}{K} \tag{63}$$

$$\frac{1}{L - x_s^*} \int_{x_s^*}^{L} \left[\sigma(x_s) - \theta(x_s) \right] dx_s \approx 0.091 \times \frac{L^2}{K} \tag{64}$$

In other words, the numerical results are in good agreement with (64), but it is less so for (63).

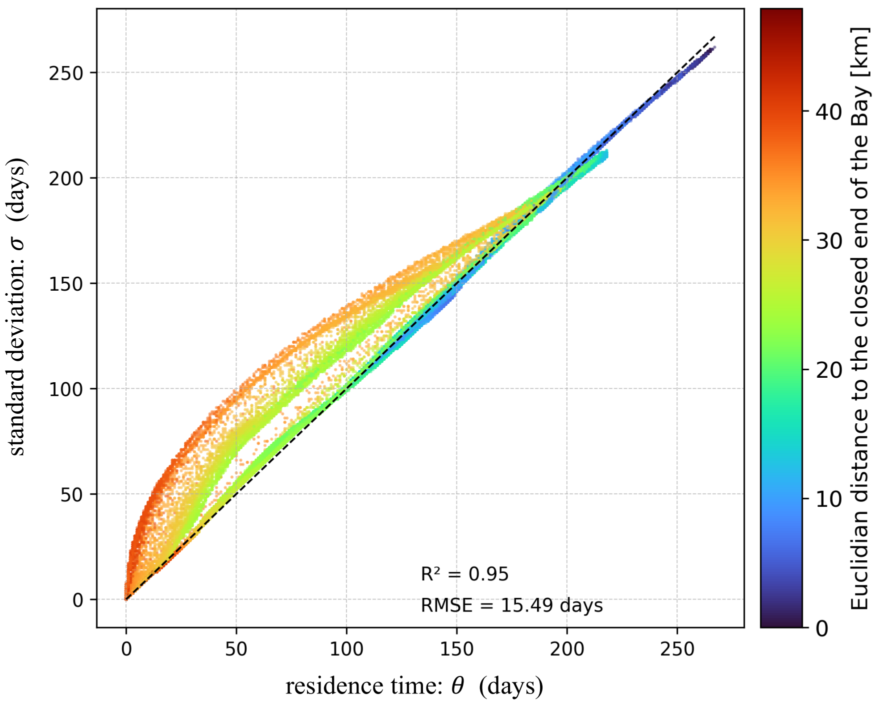

Figure 9. Scatterplot representing for each mesh (there are approximately 10^5 of them) of the Kuwait Bay numerical model of Scherpereel et al. (2025) the mean residence time (horizontal axis) and its standard deviation (vertical axis). The mean residence time and the root mean square difference between the standard deviation and the residence time are about 95.6 days and 15.49 days, respectively.

Conclusion

We failed to explain convincingly why, in each mesh of the Kuwait Bay model (Scherpereel et al. 2025), the numerically simulated residence time and its standard deviation are very close to each other. However, in the highly idealised, one-dimensional, purely diffusive model developed herein the aforementioned timescales scale in the same way and their difference is rather small, but not as small as in the numerical simulation. This suggests that at the scale of the bay transport processes are essentially of a diffusive nature.

Many aspects of the idealised model have been explored in detail and, presumably, a few novel results have been established. Unfortunately, it is uneasy to unequivocally pinpoint them in the jungle of the diagnostic timescale publications, which was half-jokingly referred to as the Tower of Babel by Viero and Defina (2016). Nonetheless, the study of Dronkers and Zimmerman (1982), however cryptic it may be, deserves to be put forward.

The one-dimensional, purely diffusive model admitting analytical solutions should not be mistaken for a compartment model (i.e., a well-mixed box model) despite the fact that these two models share some characteristics (e.g., the exponential decrease of the mass of a passive tracer in the absence of a source). The former model relies on a single characteristic timescale (i.e., the ratio of the square of the domain size to the diffusivity), whereas the functioning of the second one cannot be fully comprehended without having recourse to two timescales. These are the timescale characterising mixing within the domain of interest and the timescale associated with the flux toward the environment of the domain. If the former timescale is much smaller than the latter, mixing within the domain is often assumed to take place instantaneously. In appendix F, we show that there actually exists a spectrum of diffusive models. At one end of the spectrum, is the perfectly-mixed box model whilst, at the other end, lies a model of the same type as that investigated above.

Appendix A

We aim to demonstrate that concentration $C(t,x)$ that is governed by (1)-(4) is non negative. This is tantamount to proving that the negative part of the concentration

$$C_{-}(t,x) = \frac{C(t,x)-|C(t,x)|}{2} = \begin{cases} 0 \text{ if } C(t,x) \geq 0 \\ C(t,x) \text{ if } C(t,x) < 0 \end{cases} \tag{A.1}$$

is zero at any time $t \geq 0$. We multiply (1) by C_{-} and, after some manipulations, we obtain

$$\underbrace{\frac{d}{dt}\overbrace{\int_0^L |C_{-}|^2\,dx}^{L^2\text{-norm of } C_{-}}}_{\geq 0} = \underbrace{\left[2C_{-}K\frac{\partial C}{\partial x}\right]_{x=L}}_{=0,\text{ see (4)}} - \underbrace{\left[2C_{-}K\frac{\partial C}{\partial x}\right]_{x=0}}_{=0,\text{ see (3)}} + \underbrace{\int_0^L \left(-2K\left|\frac{\partial C_{-}}{\partial x}\right|^2\right)dx}_{\leq 0} \leq 0 \tag{A.2}$$

The L^2-norm of C_{-} is zero at $t=0$ since $C^0(x) \geq 0$ (see (2)) and, as indicated by (A.2), this norm cannot increase. Therefore, the L^2-norm of C_{-} is zero at any time, implying that, at any time and location, $C_{-}(t,x)=0$ and, hence, $C(t,x)\geq 0$. Q.E.D.

A key ingredient of the demonstration above is the assumption that diffusivity K is positive $(K>0)$. That K is a constant is unimportant in the context of the present Appendix. Indeed, if the diffusivity were a positive function of time and position, equation (1) would transform to

$$\frac{\partial C}{\partial t} = \frac{\partial}{\partial x}\left(K\frac{\partial C}{\partial x}\right) \tag{A.3}$$

with $K(t,x)>0$, and the concentration would remain non negative. This can be seen by having recourse to a line of reasoning similar to that adopted for the constant diffusivity. This kind of approach may also be resorted to for dealing with more complex partial differential problems (e.g., Blaise and Deleersnijder 2008, de Brye et al. 2012, Deleersnijder 2019b).

The mathematical developments leading to (A.2) are not as straightforward as we might think at first glance. This is because C_{-}, though continuous, is not necessarily differentiable at every point of the domain of interest. Additional pieces of information may be found in Appendix C of Deleersnijder et al. (2001) and references therein, in particular Lewandowski (1997).

Appendix B

We aim to prove that convolution product (35) is the solution to partial differential problem (1)-(4).

Substituting (35) into (1) yields

$$\begin{aligned}\frac{\partial C}{\partial t} &= \frac{\partial}{\partial t}\overbrace{\int_0^L C^0(\xi)G(t,x\,|\,\xi)\,d\xi}^{=C(t,x),\ \text{see (35)}} = \overbrace{\int_0^L C^0(\xi)\frac{\partial}{\partial t}G(t,x\,|\,\xi)\,d\xi = \int_0^L C^0(\xi)K\frac{\partial^2}{\partial x^2}G(t,x\,|\,\xi)\,d\xi}^{\text{since } \frac{\partial G}{\partial t}=K\frac{\partial^2 G}{\partial x^2},\ \text{see (36)}} \\ &= K\frac{\partial^2}{\partial x^2}\underbrace{\int_0^L C^0(\xi)G(t,x\,|\,\xi)\,d\xi}_{=C(t,x),\ \text{see (35)}} = K\frac{\partial^2 C}{\partial x^2}\end{aligned} \tag{B.1}$$

Thus, (35) satisfies partial differential equation (1). Next, at time $t=0$, (35) transforms to

$$\left[\int_0^L C^0(\xi)G(t,x\,|\,\xi)\,d\xi\right]_{t=0} = \underbrace{\int_0^L C^0(\xi)G(0,x\,|\,\xi)\,d\xi = \int_0^L C^0(\xi)\delta(x-\xi)\,d\xi}_{\text{since } G(0,x|\xi)=\delta(x-\xi),\ \text{see (37)}} = C^0(x) \tag{B.2}$$

Finally, on the boundaries of the domain, we easily obtain

$$
\begin{aligned}
\left[K\frac{\partial C}{\partial x}\right]_{x=0} &= \left[K\frac{\partial}{\partial x}\int_0^L C^0(\xi)G(t,x\,|\,\xi)\,d\xi\right]_{x=0} \\
&= \underbrace{\left[\int_0^L C^0(\xi)K\frac{\partial}{\partial x}G(t,x\,|\,\xi)\,d\xi\right]_{x=0} = 0}_{\text{since}\left[K\frac{\partial G}{\partial x}\right]_{x=0}=0\text{ , see (38)}}
\end{aligned}
\tag{B.3}
$$

and

$$
\left[C(t,x)\right]_{x=L} = \left[\int_0^L C^0(\xi)G(t,x\,|\,\xi)\,d\xi\right]_{x=L} = \underbrace{\left[\int_0^L C^0(\xi)G(t,L\,|\,\xi)\,d\xi\right]_{x=L} = 0}_{\text{since } G(t,L|\xi)=0\text{ , see (39)}}
\tag{B.4}
$$

Convolution product (35) satisfies initial and boundary conditions (2)-(4). As a consequence, (35) is the solution of partial differential problem (1)-(4). Q.E.D.

Appendix C

If $t \ll L^2/K$, the impact of the domain boundaries is small and, hence, $G(t,x\,|\,\xi)$ resembles the Green's function that would be obtained in an unbounded domain, which is hereinafter denoted $g(t,x\,|\,\xi)$. The latter is the solution of the following partial differential problem:

$$
\frac{\partial g}{\partial t} = K\frac{\partial g}{\partial x^2}
\tag{C.1}
$$

$$
\left[g(t,x\,|\,\xi)\right]_{t=0} = \delta(x-\xi)
\tag{C.2}
$$

$$
\lim_{x\to\pm\infty} g(t,x\,|\,\xi) = 0
\tag{C.3}
$$

As is well known, the solution to (C.1)-(C.3) reads (Figure C.1)

$$
g(t,x\,|\,\xi) = \frac{1}{\sqrt{4\pi Kt}}\exp\left[-\frac{(x-\xi)^2}{4Kt}\right]
\tag{C.4}
$$

As diffusion proceeds in the same manner in the direction of increasing and decreasing x, Green's function $g(t,x\,|\,\xi)$ is symmetric with respect to the point $x=\xi$:

$$
g(t,\xi+x'\,|\,\xi) = g(t,\xi-x'\,|\,\xi) \quad (x'\in]-\infty,\infty[)
\tag{C.5}
$$

In addition, as mass must be conserved, $g(t,x\,|\,\xi)$ identically satisfies

$$
\int_{-\infty}^{\infty} g(t,x\,|\,\xi)\,dx = 1
\tag{C.6}
$$

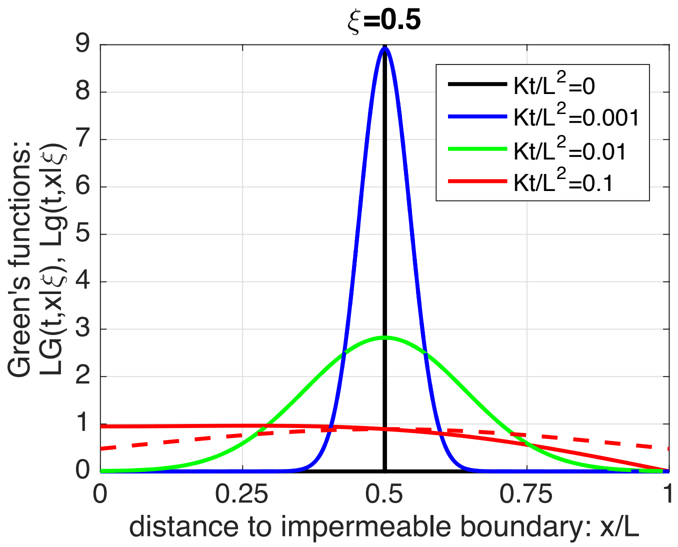

Figure C.1. Representation of Green's functions $G(t,x\,|\,\xi)$ (solid curves) and $g(t,x\,|\,\xi)$ (dashed curves) for $\xi = 0.5$ at different instant. As long as $Kt\,/\,L^2 \lessapprox 0.01$, both Green's functions are almost indistinguishable from each other. Later on, the difference between the Green's functions becomes discernible, for $G(t,x\,|\,\xi)$ is impacted by the boundaries of the domain $(x = 0, L)$, whereas this is not the case for Green's function $g(t,x\,|\,\xi)$ that is defined for $x \in]-\infty,\infty[$.

Appendix D

We aim to prove that the left hand side (LHS) of the following relations are the Fourier series of their right hand sides (RHS):

$$\frac{2}{\pi}\sum_{n=1}^{\infty}\frac{(-1)^{n+1}}{n-1/2}\cos(k_n x_s) \;=\; 1 \tag{D.1}$$

$$\frac{2L^2}{\pi^3 K}\sum_{n=1}^{\infty}\frac{(-1)^n\cos(k_n x_s)}{(n-1/2)^3} \;=\; \frac{L^2 - x_s^2}{2K} \tag{D.2}$$

$$\frac{4L^4}{\pi^5 K^2}\sum_{n=1}^{\infty}\frac{(-1)^n\cos(k_n x_s)}{(n-1/2)^5} \;=\; \frac{5L^4 - 6L^2x^2 + x^4}{12K^2} \tag{D.3}$$

To this end, it suffices to show that, for each formula, the integral over the domain of the product of the LHS and $\cos(k_n x_s)$ is equal to the integral of the product of the RHS and $\cos(k_n x_s)$. Accordingly, for $n = 1,2,3\ldots$, we obtain

$$\text{formula (D.1) : } \begin{cases} \displaystyle\int_0^L \left[\frac{2}{\pi} \sum_{n=1}^{\infty} \frac{(-1)^{n+1}}{n-1/2} \cos(k_n x_s) \right] \cos(k_n x_s)\, dx_s = \frac{L(-1)^{n+1}}{\pi(n-1/2)} \\ \displaystyle\int_0^L \cos(k_n x_s)\, dx_s = \frac{L(-1)^{n+1}}{\pi(n-1/2)} \end{cases} \tag{D.4}$$

$$\text{formula (D.2) : } \begin{cases} \displaystyle\int_0^L \left[\frac{2L^2}{\pi^3 K} \sum_{n=1}^{\infty} \frac{(-1)^n \cos(k_n x_s)}{(n-1/2)^3} \right] \cos(k_n x_s)\, dx_s = \frac{L^3(-1)^{n+1}}{\pi^3 K(n-1/2)^3} \\ \displaystyle\int_0^L \left(\frac{L^2 - x_s^2}{2K} \right) \cos(k_n x_s)\, dx_s = \frac{L^3(-1)^{n+1}}{\pi^3 K(n-1/2)^3} \end{cases} \tag{D.5}$$

$$\text{formula (D.3) : } \begin{cases} \displaystyle\int_0^L \left[\frac{4L^4}{\pi^5 K^2} \sum_{n=1}^{\infty} \frac{(-1)^n \cos(k_n x_s)}{(n-1/2)^5} \right] \cos(k_n x_s)\, dx_s = \frac{2L^5(-1)^{n+1}}{\pi^5 K^2(n-1/2)^5} \\ \displaystyle\int_0^L \left(\frac{5L^4 - 6L^2 x_s^2 + x_s^4}{12K^2} \right) \cos(k_n x_s)\, dx_s = \frac{2L^5(-1)^{n+1}}{\pi^5 K^2(n-1/2)^5} \end{cases} \tag{D.6}$$

Q.E.D.

Appendix E

We aim to establish the ordinary differential problems governing all of the moments of residence time distribution function $\mu(t,x_s)$ in the framework of the highly idealised Kuwait Bay tracer transport model.

Seeking inspiration in Bolin and Rodhe (1973), Delhez et al. (1999), Holzer and Hall (2000), Delhez and Deleersnijder (2002), Delhez et al. (2004) and Haine et al. (2025), $\mu(t,x_s)$ can be seen to obey partial differential equation (PDE)

$$\frac{\partial \mu}{\partial t} = K \frac{\partial^2 \mu}{\partial x_s^2} \tag{E.1}$$

This PDE is to be solved under initial condition

$$\left[\mu(t,x_s) \right]_{t=0} = 0 \tag{E.2}$$

and boundary conditions

$$\left[K \frac{\partial \mu}{\partial x_s} \right]_{x_s=0} = 0 \tag{E.3}$$

$$\left[\mu(t,x_s)\right]_{x_s=L} = \delta(t-0) \tag{E.4}$$

Table E.1. Analytical expressions of the first five moments of the residence time distribution function, $\gamma_j(x_s)$ $(j=0,1,\dots 4)$. The latter are evaluated by means formula (E.9).

order of the moment: j	moment: $\gamma_j(x_s)$
$j=0$	$\gamma_0(x_s) = 1$
$j=1$	$\gamma_1(x_s) = \dfrac{L^2-x_s^2}{2K}$
$j=2$	$\gamma_2(x_s) = \dfrac{5L^4-6L^2x_s^2+x_s^4}{12K^2}$
$j=3$	$\gamma_3(x_s) = \dfrac{61L^6-75L^4x_s^2+15L^2x_s^4-x_s^6}{120K^3}$
$j=4$	$\gamma_4(x_s) = \dfrac{1385L^8-1708L^6x_s^2+350L^4x_s^4-28L^2x_s^6+x_s^8}{1680K^4}$

Boundary condition (E.4) is difficult to deal with. This is why is probably easier to derive first step response $\eta(t,x_s)$, whose time derivative is the impulse response, i.e., $\mu(t,x_s)=\partial\eta(t,x_s)/\partial t$. The step response is governed by the following partial differential problem

$$\frac{\partial\eta}{\partial t}=K\frac{\partial^2\eta}{\partial x_s^2}= \quad , \quad \left[\eta(t,x_s)\right]_{t=0}=0 \quad , \quad \left[K\frac{\partial\eta}{\partial x_s}\right]_{x_s=0}=0 \quad , \quad \left[\eta(t,x_s)\right]_{x_s=L}=1 \tag{E.5}$$

whose solution reads

$$\eta(t,x_s) = 1 - \frac{2}{\pi}\sum_{n=1}^{\infty}\frac{(-1)^{n+1}}{n-1/2}e^{-Kk_n^2t}\cos(k_nx_s) \tag{E.6}$$

Then, the time derivative of (E.6) is equal to (51), as it must be.

Evaluating the moments of (E.1)-(E.4) yields the ordinary differential problems obeyed by $\gamma_j(x_s)$, with $j=0,1,2,3...$ Then, we obtain

$$K\frac{d^2\gamma_0}{dx_s^2} = 0 \quad , \quad \left[K\frac{d\gamma_0}{dx_s}\right]_{x_s=0} = 0 \quad , \quad \left[\gamma_0(x_s)\right]_{x_s=L} = 1 \tag{E.7}$$

and

$$K\frac{d^2\gamma_j}{dx_s^2} = -j\gamma_{j-1} \ , \quad \left[K\frac{d\gamma_j}{dx_s}\right]_{x_s=0} = 0 \ , \quad \left[\gamma_j(x_s)\right]_{x_s=L} = 0 \ , \quad j=1,2,3... \tag{E.8}$$

For $j=0,1,2$, the solutions are, as expected, equivalent to those obtained above by explicitly evaluating the moments of the residence time distribution function. We have not been able to derive the general expression of the moments for any value of *j*. Nonetheless, it is readily seen that they are polynomials satisfying

$$\gamma_j(x_s) = \frac{j}{K}\int_{x_s}^{L}\left(\int_0^{x_s'}\gamma_{j-1}(x_s'')dx_s''\right)dx_s' \ , \quad j=1,2,3... \tag{E.9}$$

with $\gamma_0(x_s)=1$ (Table E.1, Figure E.1).

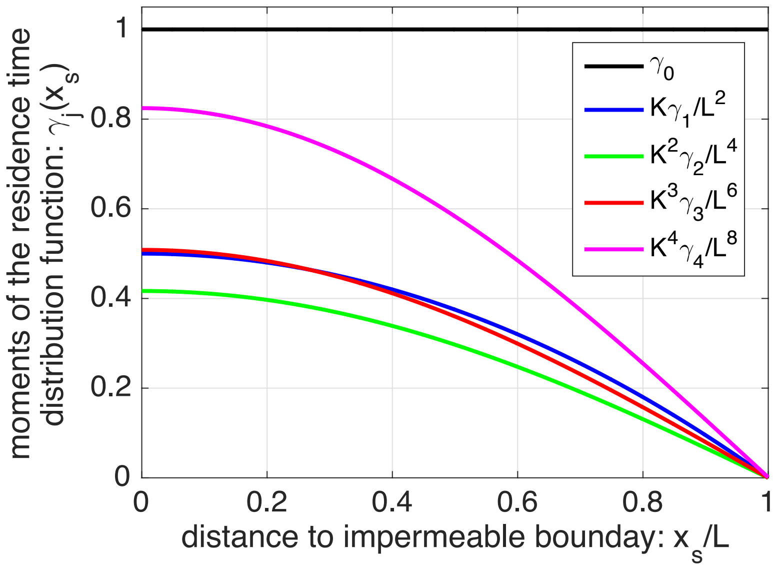

Figure E.1. Illustration of the first five moments of the residence time distribution function, i.e., $\gamma_j(x_s)$ $(j=0,1,...4)$. The analytical expressions of them are provided in Table E.1. The physical dimension of every moment is $(time)^j$.

Appendix F

In this Appendix, we will outline a one-dimensional, purely diffusive transport model that relies on two timescales so that it can behave asymptotically either as a well-mixed box model or the idealised Kuwait Bay model developed in this working note.

Let the concentration of a passive tracer, $C(t,x)$, be the solution of the following partial differential problem:

$$\frac{\partial C}{\partial t} = K\frac{\partial^2 C}{\partial x^2} \tag{F.1}$$

$$\left[C(t,x)\right]_{t=0} = C^0(x) \geq 0 \tag{F.2}$$

$$\left[K\frac{\partial C}{\partial x}\right]_{x=0} = 0 \tag{F.3}$$

$$\left[K\frac{\partial C}{\partial x} + \frac{L}{T}C\right]_{x=L} = 0 \tag{F.4}$$

where positive constant T is a timescale controlling the outgoing tracer flux. The only difference between these governing equations and (1)-(4) lies in the boundary condition prescribed at the open boundary $(x = L)$, which is now a Robin condition.

We will first demonstrate that concentration $C(t,x)$ that is governed by (F.1)-(F.4) is non negative. This is tantamount to proving that the negative part of the concentration

$$C_-(t,x) = \frac{C(t,x) - |C(t,x)|}{2} = \begin{cases} 0 \text{ if } C(t,x) \geq 0 \\ C(t,x) \text{ if } C(t,x) < 0 \end{cases} \tag{F.5}$$

is zero at any time $t \geq 0$. We multiply (F.1) by C_- and, after some manipulations, we obtain

$$\underbrace{\frac{d}{dt}\overbrace{\int_0^L |C_-|^2\,dx}^{L^2\text{-norm of } C_-}}_{\geq 0} = \underbrace{\left[2C_-K\frac{\partial C}{\partial x}\right]_{x=L}}_{\substack{=-2\frac{L}{T}\left[C_-^2\right]_{x=L}\leq 0 \\ \text{see (F.4)}}} - \underbrace{\left[2C_-K\frac{\partial C}{\partial x}\right]_{x=0}}_{=0,\text{ see (F.3)}} + \underbrace{\int_0^L\left(-2K\left|\frac{\partial C_-}{\partial x}\right|^2\right)dx}_{\leq 0} \leq 0 \tag{F.6}$$

The L^2-norm of C_- is zero at $t = 0$ since $C^0(x) \geq 0$ (see (F.2)) and, as indicated by (F.6), this norm cannot increase. Therefore, the L^2-norm of C_- is zero at any time, implying that, at any time and location, $C_-(t,x) = 0$ and, hence, $C(t,x) \geq 0$. Q.E.D.

Using Delhez et al. (2004), the pointwise residence time associated with diffusive transport model (F.1)-(F.4), $\theta(x_s)$, satisfies ordinary differential equation

$$K\frac{d^2\theta}{dx_s^2} + 1 = 0 \tag{F.7}$$

which is to be solved under boundary conditions[20]

$$\left[K\frac{d\theta}{dx_s}\right]_{x_s=0} = 0 \tag{F.8}$$

$$\left[K\frac{d\theta}{dx_s} + \frac{L}{T}\theta\right]_{x_s=L} = 0 \tag{F.9}$$

The solution to differential problem (F.7)-(F.9) reads

$$\theta(x_s) = \frac{L^2 - x_s^2}{2K} + T \tag{F.10}$$

[20] Boundary conditions (F.8) and (F.9) cannot be prescribed at our discretion. They depend on (F.3) and (F.4) as may be seen in, e.g., Delhez et al. (2004).

Clearly, this residence time is larger than (48b). This is because open boundary condition (F.9) is akin to the representation of a bottleneck, whose impact is an increasing function of timescale T. It is easily understood that the greater the value of T, the smaller the outgoing tracer flux. Residence time (F.10) exhibits two timescales, i.e., L^2 / K and T. Let their ratio be defined as follows

$$\beta = \frac{T}{L^2 / K} = \frac{\text{timescale controlling the outgoing flux}}{\text{timescale for the mixing inside the domain}} \tag{F.11}$$

Combining (F.10) and (F.11) leads to

$$\theta(x_s) = \left[\frac{1-\left(x_s / L\right)^2}{2} + \beta\right]\frac{L^2}{K} = \left[1 + \frac{1-\left(x_s / L\right)^2}{2}\frac{1}{\beta}\right]T \tag{F.12}$$

In the limit $\beta \to 0$, the impact of the aforementioned bottleneck tends to be negligible and tracer transport tends to behave as in the idealised Kuwait Bay model. On the other hand, if $\beta >> 1$, then the residence time tends to be homogeneous in the domain, which is typical of a well mixed box (e.g., Bolin and Rodhe 1973, Takeoka 1984, Deleersnijder et al. 1997, Tartinville et al. 1997, Umgiesser et al. 2014, Lucas and Deleersnijder 2020).

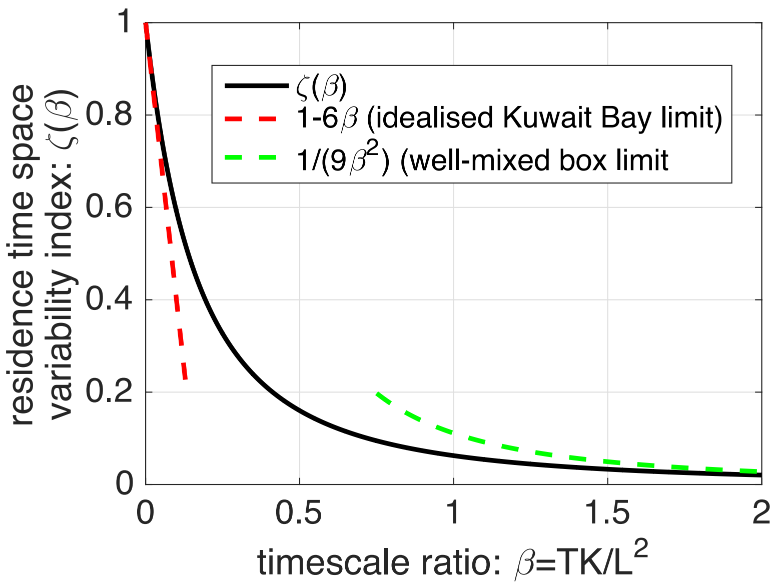

Figure F.1. Residence time space variability index (F.14) (black, solid curve) as a function of timescale ratio β, i.e., the ratio of the timescale controlling the outward flux (T) to L^2 / K, the timescale characterising diffusive processes within the domain of interest. The asymptotic behaviour in the well-mixed box limit ($\beta \to \infty$) is associated with the green, dashed curve. The red, dashed curve is associated with limit $\beta \to 0$ (negligible impact of the bottleneck at the open boundary of the domain).

The average over the domain of $\theta(x_s)$ reads

$$\langle\theta(x_s)\rangle = \frac{1}{L}\int_0^L \theta(x_s)\,dx_s = \frac{L^2}{3K} + T \tag{F.13}$$

Thus, the domain-averaged residence time simply is the sum of the mean residence time that would prevail if the were no bottleneck and the timescale controlling the outgoing flux through the bottleneck.

We introduce the following measure of the space variability of the residence time (Figure F.1)

$$\zeta(\beta) = \frac{5}{L}\int_0^L \frac{\left[\theta(x_s)-\langle\theta(x_s)\rangle\right]^2}{\langle\theta(x_s)\rangle^2}\,dx_s = \frac{1}{(1+3\beta)^2} \tag{F.14}$$

which satisfies

$$0 \le \zeta(\beta) \le 1 \tag{F15}$$

and

$$\zeta(\beta) \sim \begin{cases} 1-6\beta\,, & \beta\to 0 \ \text{(idealised Kuwait Bay limit)} \\ 1/(9\beta^2)\,, & \beta\to\infty \ \text{(well-mixed box limit)} \end{cases} \tag{F.16}$$

The lower bound, $\zeta(\infty)=0$, corresponds to a well-mixed box, whereas the upper bound, $\zeta(0)=1$ is obtained if there is no bottleneck at the open boundary (i.e., the idealised Kuwait Bay model). In other words, the smaller the value of ζ (i.e., the greater the value of dimensionless parameter β) is, the more homogeneous the residence time is.

The pointwise residence time may alo be evaluated by means of (45), which may be transformed to

$$\theta(x_s) = \int_0^L\int_0^\infty G(t,x\,|\,x_s)\,dt\,dx = \int_0^L \mathcal{G}(x\,|\,x_s)\,dx \tag{F.17}$$

with

$$\mathcal{G}(x\,|\,x_s) = \int_0^\infty G(t,x\,|\,x_s)\,dt \tag{F.18}$$

Green's function $G(t,x\,|\,x_s)$ is the solution of the following partial differential problem:

$$\begin{gathered}\frac{\partial G}{\partial t} = K\frac{\partial^2 G}{\partial x^2} \\ \left[G(t,x\,|\,x_s)\right]_{t=0} = \delta(x-x_s)\ ,\quad \left[K\frac{\partial G}{\partial x}\right]_{x=0} = 0\ ,\quad \left[K\frac{\partial G}{\partial x}+\frac{L}{T}G\right]_{x=L} = 0\end{gathered} \tag{F.19}$$

Then, the time integral of (F.19) yields the differential problem governing $\mathcal{G}(x\,|\,x_s)$, i.e.,

$$-\delta(x-x_s) = K\frac{\partial^2\mathcal{G}}{\partial x^2}\ ,\quad \left[K\frac{\partial\mathcal{G}}{\partial x}\right]_{x=0} = 0\ ,\quad \left[K\frac{\partial\mathcal{G}}{\partial x}+\frac{L}{T}\mathcal{G}\right]_{x=L} = 0 \tag{F.20}$$

which is obtained under constraint

$$\lim_{t\to\infty} G(t,x\,|\,x_s) = 0 \tag{F.21}$$

This relation may be derived by manipulating (F.19). At $x = x_s$, $\mathcal{G}(x \mid x_s)$ satisfies matching conditions

$$\left[\mathcal{G}(x \mid x_s)\right]_{x=x_s^-}^{x=x_s^+} = 0 \quad , \quad \left[K \frac{\partial \mathcal{G}}{\partial x}\right]_{x=x_s^-}^{x=x_s^+} = -\int_{x_s^-}^{x_s^+} \delta(x - x_s)\, dx \;=\; -1 \tag{F.22}$$

The solution to (F.20) and (F.22) is

$$\mathcal{G}(x \mid x_s) \;=\; \begin{cases} \dfrac{L - x_s}{K} + \dfrac{T}{L}, & 0 \le x < x_s \\ \dfrac{L - x}{K} + \dfrac{T}{L}, & x_s < x \le L \end{cases} \tag{F.23}$$

Finally, substituting (F.23) into (F.17) yields residence time (F.10) as expected.

In summary, we have seen above that the pointwise residence time may be obtained from the adjoint problem (e.g., Delhez et al. 2004) or from a simplified version of the forward method that does not require the explicitly evaluation of the Green's function (e.g., Deleersnijder et al. 2006).

Needless to say, the results obtained in this Appendix are another compelling illustration of the effectiveness of George Green's seminal work.

References

Alosairi Y. and T. Pokavanich, 2017, Seasonal circulation assessments of the Northern Arabian/Persian Gulf", *Marine Pollution Bulletin*, 116, 270–290

Alosairi Y., T. Pokavanich and N. Alsulaiman, 2018, Three-dimensional hydrodynamic modelling study of reverse estuarine circulation: Kuwait Bay, *Marine Pollution Bulletin* 127, 82–96

Andutta F.P., F. Helfer, L.B. de Miranda, E. Deleersnijder, C.J. Thomas and C. Lemckert, 2016, An assessment of transport timescales and return coefficient in adjacent tropical estuaries, *Continental Shelf Research*, 124, 49-62

Blaise S. and E. Deleersnijder, 2008, Improving the parameterisation of horizontal density gradient in one-dimensional water column models for estuarine circulation, *Ocean Science*, 4, 239-246

Bolin B. and H. Rodhe, 1973, A note on the concepts of age distribution and transit time in natural reservoirs, *Tellus*, 25, 58-62

Carslaw H.S., 1921 (2nd ed.), *Introduction to the Mathematical Theory of the Conduction of Heat in Solids*, Macmillan, 268 pages

Cox M.D., 1989, An idealized model of the World Ocean. Part I: The global-scale water masses, *Journal of Physical Oceanography*, 19, 1730-1752

de Brauwere, B. de Brye, S. Blaise and E. Deleersnijder, 2011, Residence time, exposure time and connectivity in the Scheldt Estuary, *Journal of Marine Systems*, 84, 85-95 de Brye B., A. de Brauwere, O. Gourgue, E.J.M. Delhez and E. Deleersnijder, 2012, Water renewal timescales in the Scheldt Estuary, *Journal of Marine Systems*, 94, 74-86

Deleersnijder E., 2011, *Toward a generic method to estimate the water renewal rate of a semi-enclosed domain*, Working note, Université catholique de Louvain, Louvain-la-Neuve, Belgium, 46 pages, available at URL https://hdl.handle.net/2078.5/55958

Deleersnijder E., 2016, *On some properties of steady-state partial water ages in the World Ocean*, Working note, Université catholique de Louvain, Louvain-la-Neuve, Belgium, 16 pages, available at URL http://hdl.handle.net/2078.1/176922

Deleersnijder E., 2017, *Tracking water masses when water parcels are motionless*, Working note, Université catholique de Louvain, Louvain-la-Neuve, Belgium, 7 pages, available at URL http:// hdl.handle.net/2078.1/191881

Deleersnijder E., 2019a, *A note on the estimation of orders of magnitude in marine sciences*, Working Note, Université catholique de Louvain, Louvain-la-Neuve, Belgium, 3 pages, available on the web at URL https://hdl.handle.net/2078.5/63074

Deleersnijder E., 2019b, *Water renewal of a region of freshwater influence (ROFI): mathematical properties of some of the relevant diagnostic variables*, Working Note, Université catholique de Louvain, Louvain-la-Neuve, Belgium, 19 pages, available on the web at URL http://hdl.handle.net/2078.1/220841

Deleersnijder E., 2020, *The uneasy collaboration of Leonhard Euler (1707-1783) and Joseph Louis de Lagrange (1736-1813) in environmental fluid mechanics*, Working Note, Université catholique de Louvain, Louvain-la-Neuve, Belgium, 5 pages, available on the web at URL http://hdl.handle.net/2078.1/229071

Deleersnijder E., 2025*, On the fraction of the water age accounted for by partial ages*, Working Note, Université catholique de Louvain, Louvain-la-Neuve, Belgium, 15 pages, available on the web at URL http://hdl.handle.net/2078.1/304477

Deleersnijder E., 2026, Water renewal diagnostic timescales in the river-sea continuum: outline of the theoretical underpinning and analytical solutions for an idealised channel (in preparation)

Deleersnijder E., J.-M. Beckers and E.J.M. Delhez, 2006, The residence time of settling particles in the surface mixed layer, *Environmental Fluid Mechanics*, 6, 25-42

Deleersnijder E., J.-M. Campin and E.J.M. Delhez, 2001, The concept of age in marine modelling: I. Theory and preliminary model results, *Journal of Marine Systems*, 28, 229-267

Deleersnijder E., I. Draoui, J. Lambrechts, V. Legat and A Mouchet, 2020, Consistent boundary conditions for age calculations, *Water*, 12, 1274, doi: 10.3390/w12051274

Deleersnijder A., A. Mouchet, E.J.M. Delhez and J.-M. Beckers, 2002, Transient behaviour of water ages in the World Ocean, *Mathematical and Computer Modelling*, 36, 121-127

Deleersnijder E., B. Tartinville and J. Rancher, 1997, A simple model of the tracer flux from the Mururoa Lagoon to the Pacific, *Applied Mathematics Letters*, 10(5), 13-17, doi: 10.1016/s0893-9659(97)00076-1

Delhez E.J.M., J.-M. Campin, A.C. Hirst and E. Deleersnijder, 1999, Toward a general theory of the age in ocean modelling, *Ocean Modelling*, 1, 17-27

Delhez E.J.M. and E. Deleersnijder, 2002, The concept of age in marine modelling: II. Concentration distribution function in the English Channel and the North Sea, *Journal of Marine Systems,* 31, 279-297

Delhez E.J.M., A.W. Heemink and E. Deleersnijder, 2004, Residence time in a semi-enclosed domain from the solution of an adjoint problem, *Estuarine, Coastal and Shelf Science*, 61, 691-702

Dewals B., P. Archambeau, M. Bruwier, S. Erpicum, M. Pirotton, T. Adam, E.J.M. Delhez and E. Deleersnijder, 2020, Age of water particles as a diagnosis of steady-state flows in shallow rectangular reservoirs, *Water*, 12, 2819

Dewals B., P. Archambeau, S. Erpicum, M. Pirotton and E. Deleersnijder, 2024, What does the volume-averaged water age distribution function reveal about flow fields in rectangular shallow reservoirs?, *Environmental Fluid Mechanics*, 24, 75-93

Dronkers J. and J.T.F. Zimmerman, 1982, Some principles of mixing in tidal lagoons, *Oceanologica Acta*, Numéro Spécial, Actes du Symposium International sur les lagunes côtières, SCOR/IABO/UNESCO, Bordeaux, 8-14 Septembre 1981, pages 107-117, https://archimer.ifremer.fr/doc/00246/35736/34244.pdf

Duffy D.G., 2018 (2nd. ed.), *Green's Functions with Applications*, CRC Press, Boca Raton USA, 667 pages

Goosse H., J.-M. Campin and B. Tartinville, 2001, The source of Antarctic bottom water in a global ice-ocean model, *Ocean Modelling*, 3, 51-65

Gourgue O., E. Deleersnijder and L. White, 2007, Toward a generic method for studying water renewal, with application to the epilimnion of Lake Tanganyika, *Estuarine, Coastal and Shelf Science*, 74, 628-640

Green G., 1828, *An Essay on the Application of Mathematical Analysis to the Theories of Electricity and Magnetism*, Nottingham: printed for the author by T. Wheelhouse, 72 pages, available at URL https://books.google.be/books?id=GwYXAAAAYAAJ

Haine T.W.N., S.M. Griffies, G. Gebbie and W. Jiang, 2025, A review of Green's function methods for tracer timescales and pathways in ocean models, *Journal of Advances in Modeling Earth Sytems*, 17, e2024MS004637

Haine T.W.N. and T.M. Hall, 2002, A generalized transport theory: water-mass composition and age, *Journal of Physical Oceanography*, 32, 1932-1946

Hall T.M., T.W.N. Haine, M. Holzer, D.A. LeBel, F. Terenzi and D.W. Waugh, 2007, Ventilation rates estimated from tracers in the presence of mixing, *Journal of Physical Oceanography*, 37, 2599-2611

Heemink A., E. Deleersnijder, S.H.A.M. Shah and U. Gräwe, 2022, Lagrangian modelling of transport phenomena using stochastic differential equations, in: Schuttelaars H., A. Heemink and E. Deleersnijder (Eds.), *The Mathematics of Marine Modelling — Water, Solute and Particle Dynamics in Estuaries and Shallow Seas*, Mathematics of Planet Earth

(Volume 9), Springer Nature, pages 213-242

Hirst A.C., 1999, Determination of water component age in ocean models: application to the fate of North Atlantic Deep Water, *Ocean Modelling*, 1, 81-94

Holzer M. and T.M. Hall, 2000, Transit-time and tracer-age distributions in geophysical flows, *Journal of the Atmospheric Sciences*, 57, 3539-3558

Jackson J.D., 1962 (3rd ed.), *Classical Electrodynamics*, John Wiley & Sons, New York, USA, 641 pages

Lewandowski R., 1997, *Analyse Mathématique et Océanographie*, Masson, Paris, 304 pages

Lucas L.V. and E. Deleersnijder, 2020, Timescale methods for simplifying, understanding and modeling biophysical and water quality processes in coastal aquatic ecosystems: a review, *Water*, 12, 2717, doi: 10.3390/w12102717

Meier H.E.M., 2005, Modeling the age of Baltic Seawater masses: Quantification and steady state sensitivity experiments, *Journal of Geophysical Research*, 110, C02006, doi: 10.1029/2004JC002607

Monsen N.E., J.E. Cloern, L.V. Lucas and S.G. Monismith, 2002, A comment on the use of flushing time, residence time, and age as transport time scales, *Limnology and Oceanography*, 47, 1545-1553

Pham Van C., B. de Brye, A. de Brauwere, A.J.F. Hoitink, S. Soares-Frazao and E. Deleersnijder, 2020, Numerical simulation of water renewal timescales in the Mahakam Delta, Indonesia, *Water*, 12, 1017, doi: 10.3390/w12041017

Pous S., X. Carton and P. Lazure, 2013, A process study of the wind-induced circulation in the Persian Gulf, *Open Journal of Marine Science*, 3, 1-11

Primeau F.W. and M. Holzer, 2006, The ocean's memory of the atmosphere: residence-time and ventilation-rate distributions of water masses, *Journal of Physical Ocanography*, 36, 1439-1456

Scherpereel C., Y. Alosairi, J. Lambrechts and E. Hanert, 2025, Hydrodynamic impact of bridge construction and land reclamation on water residence time and flushing processes in Kuwait Bay, *Marine Pollution Bulletin*, 214, 117716

Takeoka H., 1984, Fundamental concepts of exchange and transport time scales in a coastal sea, *Continental Shelf Research*, 3, 311-326

Tartinville B., E. Deleersnijder and J. Rancher, 1997, The water residence time in the Mururoa atoll lagoon: sensitivity analysis of a three-dimensional model, *Coral Reefs*, 16, 193-203

Umgiesser G., C. Ferrarin, A. Cucco, F. De Pascalis, D. Bellafiore, M. Ghezzo and M. Bajo, 2014, Comparative hydrodynamics of 10 Mediterranean lagoons by means of numerical modelling, *Journal of Geophysical Research: Oceans*, 119, 2212-2226, doi: 10.1002/2013JC009512

van Sebille E., S.M. Griffies, R. Abernathey, T.P. Adams, P. Berloff, A. Biastoch, B. Blanke, E.P. Chassignet, Y. Cheng, C.J. Cotter, E. Deleersnijder, K. Döös, H. Drake, S. Drijfhout, S.F. Gary, A.W. Heemink, J. Kjellsson, I.M. Koszalka, M. Lange, C. Lique, G.A.

MacGilchrist, R. Marsh, C.G. Mayorga Adame, R. McAdam, F. Nencioli, C.B. Paris, M.D. Piggott, J.A. Polton, S. Rühs, S.H.A.M. Shah, M.D. Thomas, J. Wang, P.J. Wolfram, L. Zanna and J.D. Zika, 2018, Lagrangian ocean analysis: fundamentals and practices, *Ocean Modelling*, 121, 49-75

Viero D.P. and A. Defina, 2016, Renewal time scales in tidal basins: climbing the Tower of Babel, in: *Sustainable Hydraulics in the Era of Global Change*, S. Erpicum et al. (Eds.), Taylor & Francis Group, London, pages 338-345

Yamamoto T., R. Madhusoodhanan, T. Al-Said, A. Ahmed, L. Fernandes, M. Nithyanandan, F. Thuslim, A. Alghunaim, W. Al-Zekri, S.W.A. Naqvi and F. Al-Yamani, 2022, Dynamic hydrographic and water-quality variations in the northwestern Arabian Gulf, a sinking zone of reverse estuarine circulation, *Marine Pollution Bulletin*, 179, 113714

Zimmerman J.T.F., 1976, Mixing and flushing of tidal embayments in the western Dutch Wadden Sea. Part I: Distribution of salinity and calculation of mixing time scales, *Netherlands Journal of Sea Research*, 10, 149-191

Zimmerman J.T.F., 1988, Estuarine residence times, in: *Hydrodynamics of Estuaries*, Volume I, B. Kjerfve (editor), CRC Press, pages 75-84